Systematic study on the pressure dependence of M_2AlC phases (M=Ti,V,Cr,Zr,Nb,Mo,Hf,Ta,W)

J. Emmerlich,[1,*] D. Music,[1] A. Houben,[2] R. Dronskowski,[2] and J. M. Schneider[1]
[1]*Materials Chemistry, RWTH Aachen University, Kopernikusstrasse 16, D-52074 Aachen, Germany*
[2]*Institute of Inorganic Chemistry, RWTH Aachen University, Landoltweg 1, D-52074 Aachen, Germany*
(Received 29 May 2007; published 21 December 2007)

The compressibility of the nanolaminated M_2AlC phases (space group $P6_3/mmc$) with M=Ti,Zr,Hf [valence electron concentration (VEC) of the M element of 4], V, Nb, Ta (VEC=5), and Cr, Mo, W (VEC=6) is systematically studied in the pressure range from 0 to ~70 GPa using *ab initio* calculations. These phases are characterized by interleaving of MC and Al layers. For VEC=4, we observe a larger compressibility along the c axis as compared to the a axis. As the VEC is increased to 5, the compressibility in the c direction decreases and becomes comparable to the compressibility in the a direction, whereas at VEC=6, the compressibility in the a direction is larger than that along the c direction. These results are consistent with recent experimental work. Based on a systematic study of the VEC-induced changes in bond stiffness, bond angle, and bond energy, we conclude that the geometric alteration of the bonding configuration in combination with the increase in M–C bond stiffness is mainly responsible for the observed compressibility change.

DOI: 10.1103/PhysRevB.76.224111 PACS number(s): 61.50.Lt, 62.50.+p, 71.15.Nc

INTRODUCTION

M_2AlC phases with M=Ti, V, Cr, Zr, Nb, Mo, Hf, Ta, and W belong to a family of ternary compounds (space group $P6_3/mmc$, prototype Cr_2AlC) consisting of an early transition metal (M), a group-A element (A) (mainly IIIA and IVA), and C and/or N (X) with the general formula of $M_{n+1}AX_n$ (n=1–3). The majority of these phases exhibit a stoichiometry of M_2AX and they are therefore called "211." Much attention has been drawn toward *MAX* phases owing to their unusual set of properties. They combine metallic properties, such as low electrical and thermal resistivities[1–3] as well as high ductility,[4,5] with desired ceramic characteristics of high stiffness[3,6] and resistance against oxidation.[1]

211 phases are characterized by A layers weakly bonded to M_2C blocks.[1] Recently, Nb_2AsC was experimentally subjected to hydrostatic pressure up to 41 GPa (Ref. 7) with the surprising result that the compressibility along the c axis was lower compared to that along the a axis. Similar pressure experiments on Ti_2AlC, V_2AlC, Cr_2AlC, Nb_2AlC, and Ta_2AlC (Ref. 8) revealed that the compressibility in the c direction was also lower compared to that along a for Cr_2AlC and Nb_2AlC. It was suggested that M–C and M–Al bonds are of comparable strength in M_2AlC with M=Cr,Nb,Ta.[8] However, this is inconsistent with reports indicating that *MAX* phases generally exhibit M–X bonds which are stronger than M–A bonds.[9,10]

In this paper, we present a detailed and systematic theoretical study on the compressibility of M_2AlC (M=Ti, V, Cr, Zr, Nb, Mo, Hf, Ta, and W) phases in the pressure range 0 to ~70 GPa. Variations in the unit-cell dimensions, bond lengths, bond directions, and bond energies are analyzed using *ab initio* calculations. As expected, for a valence electron concentration (VEC) of the M element of 4, the compressibility in the c direction is larger compared to that in the a direction and decreases with higher VEC. Hence, the apparent contradictive compression behavior of certain *MAX* phases reported in the literature can be understood based on the valence-electron-induced changes in bond geometry and M–C bond energy discussed here. This sheds light on unresolved questions regarding the high-pressure deformation of the *MAX* phases.

CALCULATION DETAILS

The performed calculations are based on density-functional theory (DFT) using the Vienna *ab initio* simulation program[11–13] (VASP) with projector augmented wave potentials, including the generalized-gradient approximation. The integration in reciprocal space was carried out by applying a Monkhorst-Pack scheme[14] with an energy cutoff of 500 eV and k-point grid of $7\times7\times7$. The unit-cell descriptions of the M_2AC phases of interest were based on Cr_2AlC as a prototype.[15] All equilibrium volumes and bulk moduli of the investigated M_2AlC phases were estimated from least-squares fits of the calculated energy-volume curves using the Birch-Murnighan equation of state.[16] Hydrostatic pressure on the phases was realized by a stepwise reduction of the unit-cell volume down to 25%, thus simulating a pressure variation between 0 and ~70 GPa.

Analysis of chemical bonding was performed for M_2AlC with M=Ti, V, and Cr using the tight-binding linear muffin-tin orbital method.[17–19] The program used was TB-LMTO-ASA 4.7 (Ref. 20) with a scalar-relativistic Hamiltonian and atomic-sphere approximation. The total energies were calculated based on DFT using the parametrization by Vosko *et al.*[21] augmented with gradient correction.[22] Then, the crystal orbital Hamilton population (COHP) analysis was applied,[23] which partitions the band-structure energy (sum of the Kohn-Sham eigenvalues) with respect to atomic and bonding contributions.[24] The integrated COHP (ICOHP) up to the Fermi level is a measure of the bond energy of a chemical bond between two atoms (interaction pair). In order to avoid empty interstitial sites in the theoretical description, all atomic spheres were enlarged to ensure full space filling using a semiautomatic procedure.

TABLE I. Cohesive energies, bulk moduli, equilibrium volumes, and cell parameters for M_2AlC phase with M=Ti, V, Cr, Zr, Nb, Mo, Ta, and W.

M_2AlC	Ti	V	Cr	Zr	Nb	Mo	Hf	Ta	W
Cohesive energy (eV/atom)	−7.86	−8.21	−8.16	−8.11	−8.88	−8.80	−8.87	−9.63	−9.59
Bulk modulus (GPa)	160 186[a]	202 201[a]	221 165[a]	144	203 209[a]	232	159	222 251[a]	262
Equilibrium volume (Å)	111.6 111.6[a]	96.7 97.0[a]	89.3 90.6[a]	140.3	117.0 116.2[a]	108.5	133.9	115.5 114.4[a]	106.9
a (Å)	3.066 3.065[a]	2.914 2.914[a]	2.849 2.857[a]	3.327	3.121 3.103[a]	3.047	3.279	3.101 3.086[a]	2.951
c/a	4.469 4.473[a]	4.510 4.526[a]	4.461 4.484[a]	4.400	4.446 4.489[a]	4.429	4.386	4.474 4.488[a]	4.802
z parameter	0.0837	0.0848	0.0846	0.0858	0.0894	0.0890	0.0874	0.0905	0.0934

[a]Reference 8.

RESULTS AND DISCUSSION

Table I contains the calculated cohesive energies, bulk moduli, and equilibrium volumes, as well as the cell parameters a and c/a. Our results show generally larger bulk moduli compared to experimental work,[8] with an acceptable deviation within 10%. Only Cr_2AlC divaricates 25% from the experimentally observed value. This was reported earlier;[25,26] however, the reason for this disagreement is still under debate.

Figures 1(a)–1(c) show the evolution of the normalized axial ratios ($[c/a]/[c_0/a_0]$) as a function of pressure for M_2AlC with M=Ti,Zr,Hf [see Fig. 1(a); VEC=4], V, Nb, Ta [Fig. 1(b); VEC=5], and Cr, Mo, W [Fig. 1(c); VEC=6]. The dotted line represents $(c/a)/(c_0/a_0)=1$ (axial ratio at pressure=0). As can be seen in Fig. 1(a), the normalized axial ratios are below the dotted line, which means that these compounds are more compressible in the c direction than along the a direction. This agrees well with experimental observations on the c and a compressibilities of Ti_2AlC.[8] Initially, in Fig. 1(a), the c lattice parameter changes more than the a lattice parameter (negative slope of the curve). At pressures above ~30 GPa, however, a positive slope can be observed which eventually reaches $(c/a)/(c_0/a_0)\approx 1$ at ~60 GPa. This is representative of all studied M_2AlC phases with VEC=4. Furthermore, *ab initio* compressibility data of Ti_3SiC_2 (Refs. 27 and 28) show similar behavior at pressures above ~40 GPa, which was correlated to modifications in the interatomic distance between the Ti and Si basal planes.

A different behavior is observed in Fig. 1(b), where $(c/a)/(c_0/a_0)$ is plotted versus pressure for M_2AlC with M=V, Nb, and Ta (VEC=5). Nb_2AlC and Ta_2AlC behave similarly under compression, in the sense that the normalized lattice-parameter ratios vary around unity. For V_2AlC, the variation is larger and becomes more significant at higher pressures, where a positive slope is observed. A compressibility that is similar in the a and c directions, as observed in this study for Ta_2AlC and Nb_2AlC, was experimentally observed only for Ta_2AlC.[8] For Nb_2AlC, a higher compressibility along the a direction as compared to the c direction and the opposite behavior for V_2AlC were experimentally determined. The discrepancy between theory (this work) and experiment in the cases of Nb_2AlC and V_2AlC (Ref. 8) may arise due to the deviation of the test specimens from perfect crystals, such as defect concentration, polycrystallinity, impurity phases, elements, etc.

In Fig. 1(c), a positive slope in the entire pressure range can be observed for all M_2AlC phases with VEC=6 (M=Cr,Mo,W). This is somewhat surprising, having in mind the anisotropic bonding nature of the M_2AX phase with

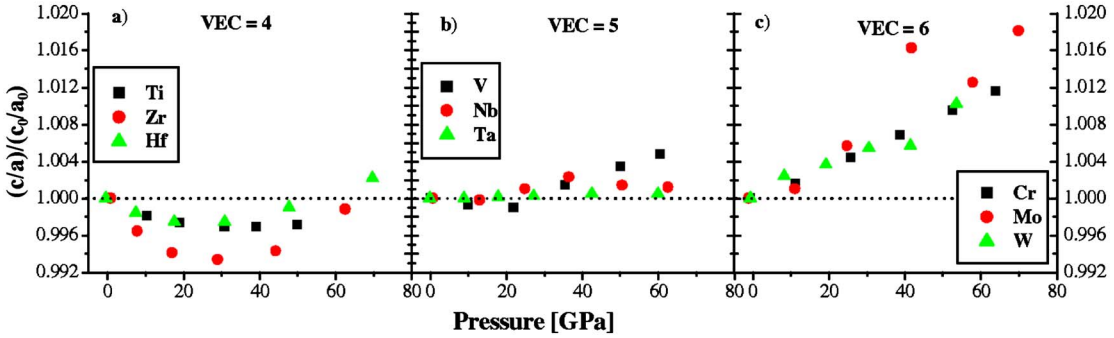

FIG. 1. (Color online) Evolution of the normalized lattice-parameter ratios ($[c/a]/[c_0/a_0]$) as a function of pressure for M_2AlC with M=(a)Ti,Zr,Hf; (b) V, Nb, Ta; (c) Cr, Mo, W.

TABLE II. Coefficients of second order polynomial fit ($y=C_0+C_1x+C_2x^2$) of relative stiffness as a function of pressure.

	$M-$Al			$M-$C		
M	C_0	$C_1\times10^{-3}$	$C_2\times10^{-5}$	C_0	$C_1\times10^{-3}$	$C_2\times10^{-6}$
Ti	1	−2.6	1.3	1	−1.4	6.5
V	1	−2.3	1.3	1	−0.9	1.3
Cr	1	−2.0	1.0	1	−1.1	4.8
Zr	1	−3.1	2.0	1	−1.5	7.3
Nb	1	−2.2	1.1	1	−1.1	3.8
Mo	1	−2.0	1.0	1	−0.9	2.7
Hf	1	−2.6	1.4	1	−1.2	4.4
Ta	1	−1.9	0.9	1	−1.2	6.6
W	1	−1.8	1.0	1	−0.9	4.0

weakly bonded A layers in between essentially covalently bonded $M-X$ blocks.[1,10,29,30] However, experimental work[8] on Cr_2AlC is consistent with our calculation results. The compressibility in the c direction is indeed smaller compared to that along the a direction. It was suggested that the $M-$Al and $M-$C bond strengths of these phases are similar.[8] Considering the general trend in Figs. 1(a)–1(c), it is apparent that with higher VEC and pressure, the compressibility of the M_2AlC phases along the c direction becomes smaller.

The electronic structure of M_2AlC phases and their elastic properties were systematically studied by Sun *et al.*,[9,31] Wang and Zhou,[10] and Music *et al.*[26,29] Sun and Music observed that the M_2AC phases can be classified into two groups: weakly coupled (VEC=4) and strongly coupled phases (VEC=5 and 6). Our compressibility results are consistent with the classification notion that the compressibility of M_2AlC phases is larger along the c direction as compared to that along the a direction for VEC=4 (weak coupling), whereas the compressibility along the c axis is equal to or smaller than that in a direction for VEC=5 and 6 (strong coupling).

In order to investigate the response of the bonds to deformation, the relative bond stiffness of $M-$Al and $M-$C bonds was estimated from the linear coefficient (C_1) of the polynomial second order fit [$f(x)=C_0+C_1x+C_2x^2$] of the change in bond length versus pressure. The coefficients from the fitted data are listed in Table II. Figures 2(a) and 2(b) show the stiffness of M-Al and $M-$C bonds relative to Ti-Al and Ti-C, respectively, as a function of VEC. In general, the stiffness of the $M-$C bonds is higher compared to that of the $M-$Al bonds. Also, a general trend of increasing stiffness with higher VEC is observed for $M-$Al and $M-$C bonds, with the exception of V-C, which may be due to harmonic effects. However, stiffness data are consistent with calculations from previous work.[25,32]

To evaluate the stiffness data from an electronic-structure point of view, the chemical bonds have been numerically analyzed using COHP. In Figs. 3(a)–3(i), the COHPs are compared as a function of energy for the $M-$C, $M-$Al, and Al-Al bonds in M_2AlC (M=Ti, V, Cr) for low (~0 GPa) and high pressures (~70 GPa) (filled curve). C-C and Al-C bond energies are not included because the interaction is small and of antibonding nature. At low pressure, the Ti-C, V-C, and Cr-C bonds (top figure) below the Fermi level are populated in the approximate ranges of −2.8 to −6.0 eV, −3.7 to −7.3 eV, and −4.2 to −8.0 eV, respectively. The lower energies and broader energy range for the $M-$C bonds with higher VEC suggest that Cr-C bonds are stronger than the Ti-C and V-C bonds. This is confirmed by the integrated COHPs (bond energies) in Ref. 30 and consistent with density of states and band-structure calculations on these 211-*MAX* phases.[9,31] Considering the $M-$C bonds at high pressure, the populated energies shift to even lower values and, therefore, strengthening occurs, which is most pronounced for Cr-C (see Table III). Similar arguments can be made for the M–Al as well as Al-Al bonds [see Figs. 3(b)–3(g) and 3(i)] because both show an increase in population with applied pressure and, thus, bond strengthening.

For the $M-$Al bonds (middle figure), states at the Fermi level are populated and even increase with pressure for Ti-Al bonds. COHPs at the Fermi level for Al-Al interactions are

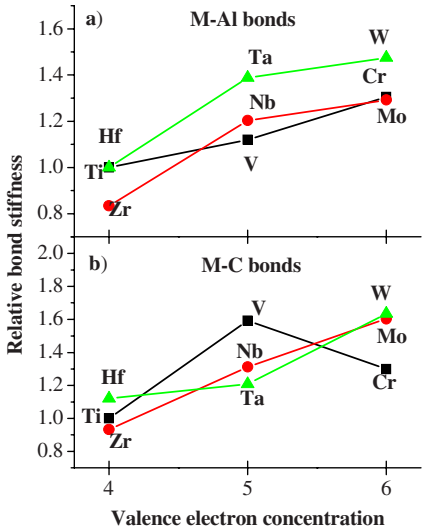

FIG. 2. (Color online) Bond stiffness of (a) $M-$Al and (b) $M-$C bonds relative to Ti-Al and Ti-C vs transition metal valence electron concentration, respectively, fitted with a second order polynomial.

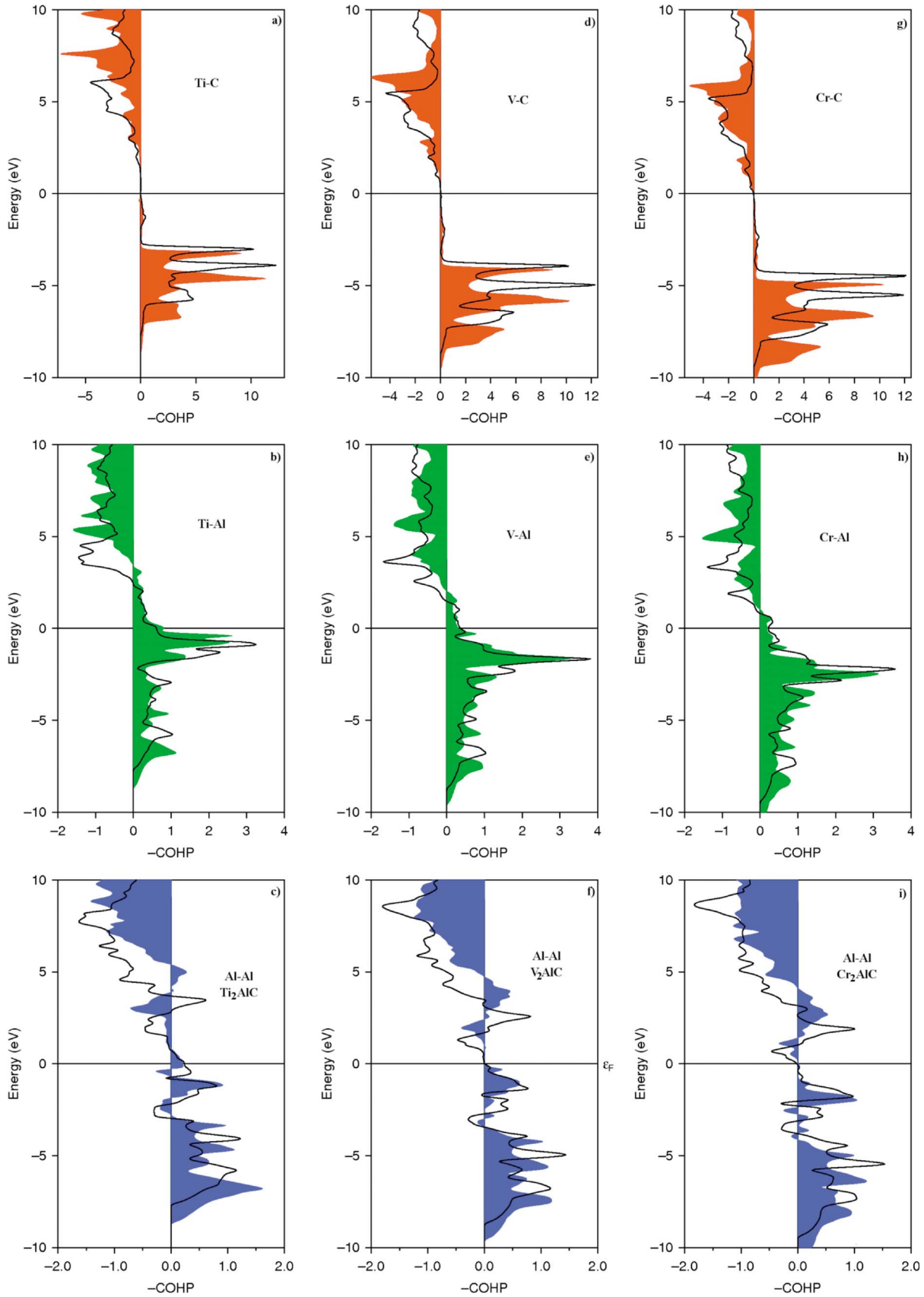

FIG. 3. (Color online) Crystal orbital Hamilton population for (a) Ti-C, (b) Ti-Al, (c) Al-Al in Ti_2AlC, (d) V-C, (e) V-Al, (f) Al-Al in V_2AlC, (g) Cr-C, (h) Cr-Al, and (i) Al-Al in Cr_2AlC. The black curves represent the COHPs at low pressure, while the filled curves result from the calculations at high pressure. Positive values in the x direction (–COHP) indicate bonding states. The Fermi energy is set to zero.

TABLE III. Energy (ICOHP) per bond (E_b) and per unit cell (E_{uc}) at low (E_{uc}^{low}) and high pressures (E_{uc}^{high}). The relative change in E_{uc} with pressure is designated as E_{uc}^{rel} and weighted with the significance E_{uc}^{weigh} of the respective bond in the unit cell, whereby positive values of E_{uc}^{rel} and E_{uc}^{weigh} indicate bond strengthening.

	Low pressure		High pressure				
	E_b (eV/bond)	E_{uc}^{low} (eV/cell)	E_b (eV/bond)	E_{uc}^{high} (eV/cell)	E_{uc}^{rel} (%/bond)	E_{uc}^{weigh} (%/cell)	
Ti-Ti$_{a\ \text{plane}}$	−0.54	−3.24	−0.55	−3.33	2.78	0.26	Ti_2AlC
Ti-Ti	−0.55	−1.64	−0.46	−1.37	−16.46	−0.78	
Ti-Al	−0.92	−5.55	−0.97	−5.80	4.50	0.72	
Al-Al	−0.57	−3.41	−0.72	−4.32	26.69	2.62	
Ti-C	−3.48	−20.88	−3.65	−21.92	4.98	3.00	
Al-C	0.03	0.20	0.03	0.20	0.00	0.00	
V-V$_{a\ \text{plane}}$	−0.69	−4.13	−0.78	−4.70	13.80	1.42	V_2AlC
V-V	−0.61	−1.82	−0.48	−1.45	−20.33	−0.92	
V-Al	−1.08	−6.49	−1.18	−7.09	9.24	1.50	
Al-Al	−0.63	−3.78	−0.73	−4.36	15.34	1.45	
V-C	−3.97	−23.84	−4.21	−25.27	6.00	3.57	
Al-C	0.03	0.20	0.03	0.19	−5.00	0.02	
Cr-Cr$_{a\ \text{plane}}$	−0.67	−4.00	0.82	−4.94	23.50	2.21	Cr_2AlC
Cr-Cr	−0.63	−1.89	0.49	−1.47	−22.22	−0.99	
Cr-Al	−1.16	−6.98	−1.30	−7.82	12.03	1.98	
Al-Al	−0.67	−3.99	−0.75	−4.48	12.28	1.15	
Cr-C	−4.27	−25.64	−4.63	−27.79	8.39	5.06	
Al-C	0.03	0.20	0.03	0.18	−10.00	0.05	

negligible except in Ti_2AlC, where a constant value of ~0.25 is calculated. It is thus reasonable to assume that the electrical conductivity may increase as pressure is applied. Additionally, for Al-Al bonds, antibonding contributions are observed, which are less significant at higher pressure.

The energies per bond (E_b) and per unit cell (E_{uc}) at low (E_{uc}^{low}) and high pressures (E_{uc}^{high}) were calculated by integrating the COHP for M_2AlC for M=Ti, V, and Cr. E_{uc} corresponds to E_b multiplied by the population of a particular bond in the unit cell. The results are summarized in Table III for pressures of ~0 and up to ~70 GPa. The relative changes of E_{uc} from low to high pressure are designated as $E_{uc}^{rel}=E_{uc}^{low}/E_{uc}^{high}$. In order to take into account not only E_{uc}^{low} but also the significance of E_{uc}^{low} in the unit cell, the E_{uc}^{rel} values are weighted (E_{uc}^{weigh}) by the ratio of $E_{uc}^{low}/\Sigma E_{uc}^{low}$. This is expressed by

$$E_{uc}^{weigh}=\frac{E_{uc}^{rel}E_{uc}^{low}}{\sum E_{uc}^{low}}. \quad (1)$$

Thus, E_{uc}^{weigh} illustrates to what extent each bond that is present in M_2AlC contributes to elastic deformation as pressure is applied. Hereby, a positive value is indicative of bond strengthening. From Table III, it can be learned that the Al-Al contribution against deformation is substantial in Ti_2AlC but decreases drastically with increasing VEC, whereas $M-M_{a\ \text{plane}}$ bonds act against this trend but to a smaller extent. Both contribute purely in the a direction, i.e., the compressibility for Cr_2AlC increases along the a axis. The data in Table III show that E_{uc}^{weigh} (M–C) is the largest compared to the remaining bonds in the unit cell and its significance increases at higher VEC. A similar trend is observed for E_{uc}^{weigh} (M–Al), but to a much smaller extent.

The ICOHP value (bond energies) of Al-C is very small and positive, which is indicative of negligible antibonding interactions. In Ref. 8 it is argued that the smaller compressibility along the c direction, as compared to that in the a direction, is a consequence of the presence of C stabilizing the M–Al bonds by preventing antibonding states. However, since the observed antibonding interaction between Al and C is negligible, we cannot supply any evidence to support this notion.[8]

Not only the bond lengths, considered through the relative stiffness, but also the bond angles are affected by the applied pressure, whereby the directionality of the respective bonds changes under pressure. Therefore, the bond angles of M with respect to the A layer (α) and the C layer (β) are calculated. The unit cell, as well as the angles α and β and their geometric relation to the basal plane, is described in Fig. 4. The changes of α and β relative to Ti_2AlC as a function of pressure are plotted in Figs. 5(a)–5(c) and Figs. 6(a)–6(c), respectively. In general, the results show that α decreases with the applied pressure and the magnitude of the change increases with VEC. In terms of directionality, this means

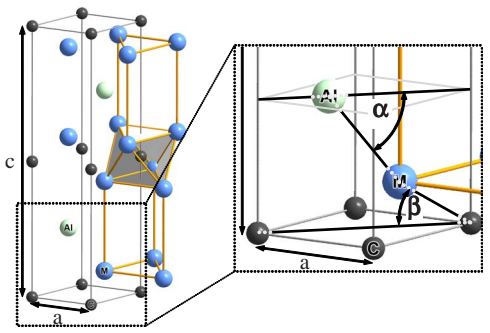

FIG. 4. (Color online) Geometric relation in the unit cell between the bond angles of Ti with respect to the Al layer (α) and the C layer (β).

that the $M-$Al bonds are aligned toward the basal plane and, thus, act more against deformation in the a direction. As it is seen from Figs. 6(a)–6(c), β increases under pressure to a larger extent compared to the soft $M-$Al bonds, resulting in a strong alignment of $M-$C bonds along the c direction. This is associated with a displacement in the c direction of the M atom away from the nearest carbon layer and infers that $M-M$ bonds are deformable, as observed for $Nb_{2-x}W_xAlC$ solid solutions[33] and Ta_2AlC.[34]Based on these findings, it is evident that the compression along the c direction is more difficult than that in the a direction as pressure is applied. The valence-electron-induced increase in $M-$C bond energy

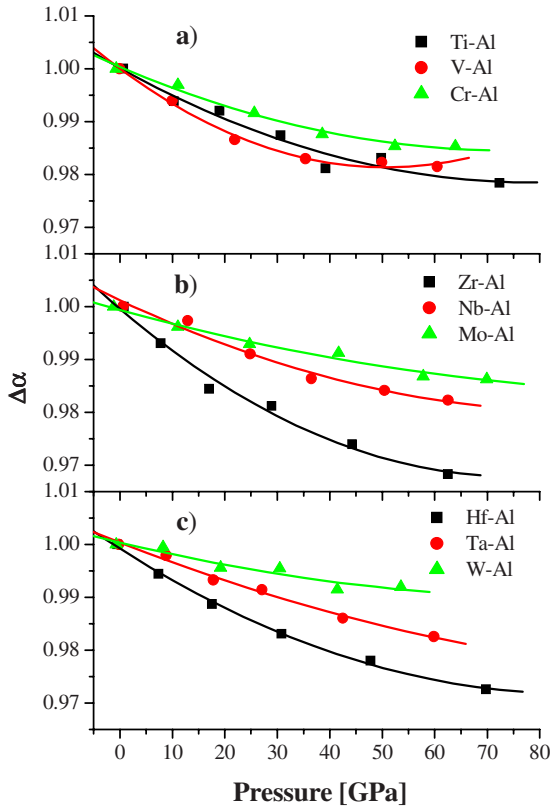

FIG. 5. (Color online) Change in $M-$Al bond angle ($\Delta\alpha$) of (a) Ti-Al, V-Al, Cr-Al relative to Ti-Al, (b) Zr-Al, Nb-Al, Mo-Al relative to Zr-Al, and (c) Hf-Al, Ta-Al, W-Al relative to Hf-Al as a function of pressure.

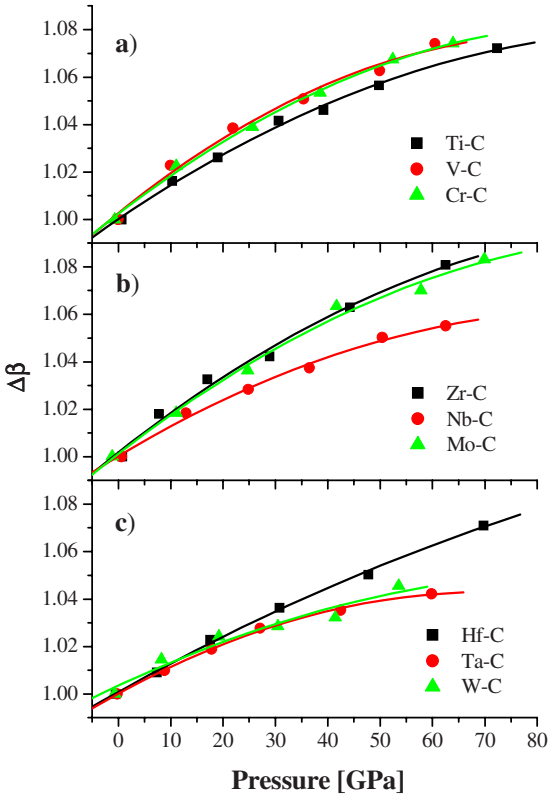

FIG. 6. (Color online) Change in $M-$C bond angle ($\Delta\beta$) of (a) Ti-Al, V-Al, Cr-Al relative to Ti-Al, (b) Zr-Al, Nb-Al, Mo-Al relative to Zr-Al, and (c) Hf-Al, Ta-Al, W-Al relative to Hf-Al as a function of pressure.

fosters this compressibility behavior. These mechanisms impart large impedance onto the compression in the c direction and imply that the compressibility along the a axis in the M_2AlC phases becomes comparable and eventually exceeds that along the c direction for VEC $\geqslant 5$.

CONCLUSIONS

In our systematic study on the compressibility of M_2AlC phases (M=Ti, V, Cr, Zr, Nb, Mo, Hf, Ta, and W) as a function of VEC in the pressure range of 0 to ~70 GPa, we calculated, as expected, a larger compressibility in the c direction than along the a direction for VEC=4. This is consistent with the notion of weaker $M-$Al bonds compressed in the c direction and stronger $M-$C bonds compressed in the a direction. However, as VEC is increased, the compressibility differences in the a and c directions decrease and at VEC =6, the compressibility in the c direction is smaller than that in the a direction. This apparent contradiction can be understood based on the valence-electron-induced changes in bond geometry and $M-$C bond energy discussed here.

For all studied phases, the M element is shifted away from the C plane closer to the Al plane as pressure is applied. This, in turn, means that $M-$C bonds are being oriented toward the c axis. With the increase in $M-$C bond stiffness as a function of VEC, the compressibility along the c axis is thus decreased at higher VEC. In addition, the study on the

bond energies and their significance in the structure showed that the Al-Al bonds become less significant in the M_2AlC phases with higher VEC. Based on these findings, it is no longer surprising that the obtained compressibility is in apparent contradiction with the anisotropic bonding structure of the M_2AlC phases. This implies that the anisotropic behavior, in terms of elasticity of the *MAX* phases in compression, may be less significant than expected for VEC $\geqslant 5$.

ACKNOWLEDGMENT

We acknowledge financial support from DFG (Schn. 735/15-1, "Adaptive Oberflächen für Hochtemperatur-Anwendungen").

*Corresponding author; emmerlich@mch.rwth-aachen.de

[1] M. W. Barsoum, Prog. Solid State Chem. **28**, 201 (2000).
[2] M. W. Barsoum, G. Yaroschuk, and S. Tyagi, Scr. Mater. **37**, 1583 (1997).
[3] J. Emmerlich, J.-P. Palmquist, Zs. Cziganý, H. Högberg, Sz. Sasvári, J.-M. Molina-Aldareguia, P. O. Å. Persson, U. Jansson, and L. Hultman, J. Appl. Phys. **96**, 4817 (2004).
[4] M. W. Barsoum and T. El-Raghy, Metall. Mater. Trans. A **33**, 363 (1999).
[5] J. M. Molina-Aldareguia, J. Emmerlich, J.-P. Palmquist, U. Jansson, and L. Hultman, Scr. Mater. **49**, 155 (2003).
[6] J. D. Hettinger, S. E. Lofland, P. Finkel, T. Meehan, J. Palma, K. Harrell, S. Gupta, A. Ganguly, T. El-Raghy, and M. W. Barsoum, Phys. Rev. B **72**, 115120 (2005).
[7] R. S. Kumar, S. Rekhi, A. L. Cornelius, and M. W. Barsoum, Appl. Phys. Lett. **86**, 111904 (2005).
[8] B. Manoun, R. P. Gulve, S. K. Saxena, S. Gupta, M. W. Barsoum, and C. S. Zha, Phys. Rev. B **73**, 024110 (2006).
[9] Z. Sun, R. Ahuja, Sa Li, and J. M. Schneider, Appl. Phys. Lett. **83**, 899 (2003).
[10] J. Wang and Y. Zhou, Phys. Rev. B **69**, 214111 (2004).
[11] W. Kohn and L. J. Sham, Phys. Rev. **140**, A1133 (1965).
[12] G. Kresse and J. Hafner, Phys. Rev. B **48**, 13115 (1993).
[13] G. Kresse and J. Hafner, Phys. Rev. B **49**, 14251 (1994).
[14] H. J. Monkhorst and J. D. Pack, Phys. Rev. B **13**, 5188 (1976).
[15] W. Jeitschko, H. Nowotny, and F. Benesovsky, Monatsh. Chem. **94**, 672 (1963).
[16] F. Birch, J. Geophys. Res. **83**, 1257 (1978).
[17] O. K. Andersen, Phys. Rev. B **12**, 3060 (1975).
[18] O. K. Andersen, *The Electronic Structure of Complex Systems*, edited by P. Phariseau and W. M. Temmerman (Plenum, New York, 1984).
[19] H. Skriver, *The LMTO Method* (Springer-Verlag, Berlin, 1984).
[20] G. Krier, O. Jepsen, A. Burkhardt, and O. K. Andersen, TB-LMTO-ASA, Version 4.7, Max-Planck-Institut für Festkörperforschung, Stuttgart, Germany.
[21] S. H. Vosko, L. Wilk, and M. Nusair, Can. J. Phys. **58**, 1200 (1980).
[22] J. P. Perdew, J. A. Chevary, S. H. Vosko, K. A. Jackson, M. R. Pederson, D. J. Singh, and C. Fiolhais, Phys. Rev. B **46**, 6671 (1992).
[23] R. Dronskowski and P. E. Blöchl, J. Phys. Chem. **97**, 8617 (1993).
[24] R. Dronskowski, *Computational Chemistry of Solid State Materials* (Wiley-VCH, Weinheim, 2005).
[25] Z. Sun, S. Li, R. Ahuja, and J. M. Schneider, Solid State Commun. **129**, 589 (2004).
[26] D. Music, Z. Sun, A. A. Voevodin, and J. M. Schneider, Solid State Commun. **139**, 139 (2006).
[27] J. Y. Wang and Y. C. Zhou, J. Phys.: Condens. Matter **15**, 1983 (2003).
[28] C. M. Fang, R. Ahuja, O. Eriksson, S. Li, U. Jansson, O. Wilhelmsson, and L. Hultman, Phys. Rev. B **74**, 054106 (2006).
[29] D. Music, Z. Sun, R. Ahuja, and J. M. Schneider, Phys. Rev. B **73**, 134117 (2006).
[30] D. Music, A. Houben, R. Dronskowski, and J. M. Schneider, Phys. Rev. B **75**, 174102 (2007).
[31] Z. Sun, D. Music, R. Ahuja, Sa Li, and J. M. Schneider, Phys. Rev. B **70**, 092102 (2004).
[32] G. Hug, Phys. Rev. B **74**, 184113 (2006).
[33] J. M. Schneider, Z. Sun, and D. Music, J. Phys.: Condens. Matter **17**, 6047 (2005).
[34] D. Music, J. Emmerlich, and J. M. Schneider, J. Phys.: Condens. Matter **19**, 136207 (2007).